In vitro selection of *Phytomonas serpens* cells resistant to the calpain inhibitor MDL28170: alterations in fitness and expression of the major peptidases and efflux pumps

SIMONE S. C. OLIVEIRA[1], INÊS C. GONÇALVES[2], VITOR ENNES-VIDAL[3], ANGELA H. C. S. LOPES[2], RUBEM F. S. MENNA-BARRETO[4], CLAUDIA M. D'ÁVILA-LEVY[3], ANDRÉ L. S. SANTOS[1,5] *and* MARTA H. BRANQUINHA[1]*

[1] *Laboratório de Investigação de Peptidases, Departamento de Microbiologia Geral, Instituto de Microbiologia Paulo de Góes (IMPG), Universidade Federal do Rio de Janeiro (UFRJ), Rio de Janeiro, Brazil*
[2] *Laboratório de Bioquímica de Microrganismos, Departamento de Microbiologia Geral, IMPG, UFRJ, Rio de Janeiro, Brazil*
[3] *Laboratório de Estudos Integrados em Protozoologia, Coleção de Protozoários, IOC, FIOCRUZ, Rio de Janeiro, Brazil*
[4] *Laboratório de Biologia Celular, Instituto Oswaldo Cruz (IOC), Fundação Oswaldo Cruz (FIOCRUZ), Rio de Janeiro, Brazil*
[5] *Programa de Pós-Graduação em Bioquímica, Instituto de Química, UFRJ, Rio de Janeiro, Brazil*

(*Received 15 March 2017; revised 11 July 2017; accepted 9 August 2017; first published online 17 October 2017*)

SUMMARY

The species *Phytomonas serpens* is known to express some molecules displaying similarity to those described in trypanosomatids pathogenic to humans, such as peptidases from *Trypanosoma cruzi* (cruzipain) and *Leishmania* spp. (gp63). In this work, a population of *P. serpens* resistant to the calpain inhibitor MDL28170 at 70 μM (MDL^R population) was selected by culturing promastigotes in increasing concentrations of the drug. The only relevant ultrastructural difference between wild-type (WT) and MDL^R promastigotes was the presence of microvesicles within the flagellar pocket of the latter. MDL^R population also showed an increased reactivity to anti-cruzipain antibody as well as a higher papain-like proteolytic activity, while the expression of calpain-like molecules cross-reactive to anti-Dm-calpain (from *Drosophila melanogaster*) antibody and calcium-dependent cysteine peptidase activity were decreased. Gp63-like molecules also presented a diminished expression in MDL^R population, which is probably correlated to the reduction in the parasite adhesion to the salivary glands of the insect vector *Oncopeltus fasciatus*. A lower accumulation of Rhodamine 123 was detected in MDL^R cells when compared with the WT population, a phenotype that was reversed when MDL^R cells were treated with cyclosporin A and verapamil. Collectively, our results may help in the understanding of the roles of calpain inhibitors in trypanosomatids.

Key words: *Phytomonas*, calpain-like proteins, calpain inhibitors, resistance, peptidases.

INTRODUCTION

Phytomonas serpens is a tomato parasite considered an important tool for biochemical and molecular studies in trypanosomatids (Jaskowska *et al*. 2015) due to its easy cultivation *in vitro* and the expression of similar molecules to those described in pathogenic species to humans, including virulence-associated ones. Among these, our research group has demonstrated the presence of a 63-kDa metallopeptidase with similarity to *Leishmania* spp. gp63, and two cysteine-type peptidases of 38 and 40 kDa that have similar antigenic properties with the major *Trypanosoma cruzi* cysteine peptidase, named cruzipain (Santos *et al*. 2007; d'Avila-Levy *et al*. 2014). This is reflected in the strong reactivity of *P. serpens* antigens with sera from Chagas' disease patients (Santos *et al*. 2007). Both proteolytic groups participate in the adhesion process of *P. serpens* to the explanted salivary glands of the phytophagous insect *Oncopeltus fasciatus* (Santos *et al*. 2007; d'Avila-Levy *et al*. 2014), which is considered an experimental model to study the interaction of the phytomonad with its invertebrate host (Jaskowska *et al*. 2015).

The characterization of calpains in trypanosomatids is a growing field of research (Branquinha *et al*. 2013). Calpains are calcium-dependent cysteine peptidases that have been originally studied in humans because calpain activation seems increased during normal aging and in many pathologies; in addition, homologues were found in a wide range of organisms (Ono and Sorimachi, 2012). The use of calpain inhibitors is demonstrably beneficial in animal models of human diseases; hence, this class of proteolytic enzyme has been proposed as a potential drug target in mammalian and non-mammalian taxa (Branquinha *et al*. 2013; Donkor, 2015). Synthetic reversible peptide calpain inhibitors, such as MDL28170, also known as calpain

* Corresponding author: Departamento de Microbiologia Geral, Instituto de Microbiologia Paulo de Góes, Universidade Federal do Rio de Janeiro, Av. Carlos Chagas Filho 373, Centro de Ciências da Saúde, 21941-902, Rio de Janeiro, Brazil. E-mail: mbranquinha@micro.ufrj.br

Parasitology (2018), **145**, 355–370. © Cambridge University Press 2017
doi:10.1017/S0031182017001561

https://doi.org/10.1017/S0031182017001561 Published online by Cambridge University Press

inhibitor III, which displays high membrane permeability (Rami *et al*. 1997), may inhibit calpains. In this sense, our group has demonstrated that MDL28170 affected many biological aspects in *T. cruzi* and *Leishmania amazonensis* life cycles (Branquinha *et al*. 2013): these studies have pointed at ultrastructural alterations (Branquinha *et al*. 2013; Marinho *et al*. 2014), fluctuations of the expression levels of calpain-like proteins (CALPs) and distinct peptidases, reduction in the adhesion to the insect midgut and in the interaction with macrophages, impairment of differentiation and viability of infective forms (Branquinha *et al*. 2013), besides the induction of apoptosis (Marinho *et al*. 2014). Moreover, addition of distinct calpain inhibitors to the culture medium of *P. serpens* led to a dose-dependent reduction in the proliferation of the parasite, being MDL28170 the most potent inhibitor (Oliveira *et al*. 2017).

Another relevant aspect in this field is the differential expression of components of the calpain family in trypanosomatid strains displaying resistance to different antimicrobials (Vergnes *et al*. 2007; Andrade *et al*. 2008; Brotherton *et al*. 2013). Drug resistance mechanisms can be promptly studied in resistant parasites obtained *in vitro* under drug pressure since a reliable comparison between the resistant strain and the parental, wild-type (WT) strain from which it was generated is provided (Andrade *et al*. 2008; Brotherton *et al*. 2013). In view of the potential use of calpain inhibitors against trypanosomatids, the aim of this study was to select a *P. serpens* population resistant to the calpain inhibitor MDL28170 by *in vitro* drug pressure and to comparatively evaluate the changes in the biology and physiology of the MDL28170-resistant parasite population, with relevance to expression of peptidases and interaction with the invertebrate host and a possible mechanism of drug resistance.

MATERIALS AND METHODS

Parasite and cultivation

Phytomonas serpens (isolate 9T), isolated from tomato (*Lycopersicon esculentum*), is deposited under the accession number COLPROT 189 at Protozoa Collection, Instituto Oswaldo Cruz – Fundação Oswaldo Cruz, Rio de Janeiro, Brazil. The plant flagellate was grown in Warren medium (3·7% brain heart infusion medium supplemented with folic acid 10 μg L^{-1} and hemin 1 mg L^{-1}) containing 5% (v/v) heat-inactivated fetal bovine serum at 28 °C for 4 days.

Calpain inhibitors

Calbiochem (San Diego, CA, USA) supplied the three cell-permeable calpain inhibitors employed in this study: MDL28170 (Z–Val–Phe–CHO; Z = *N*-benzyloxycarbonyl) is a reversible peptidomimetic inhibitor, also known as calpain inhibitor III; calpain inhibitor V (Mu-Val-HPh-FMK; Mu = morpholinoureidyl; HPh = homophenylalanyl; FMK = fluoromethylketone) is an irreversible peptidomimetic inhibitor; and PD150606 (3-(4-Iodophenyl)-2-mercapto-(Z)-2-propenoic acid) is a non-competitive calpain inhibitor directed towards the calcium-binding sites of calpain. Stock solutions were prepared in dimethylsulfoxide (DMSO; Sigma-Aldrich, Saint Louis, MO, USA) at 5 mM.

Generation of MDL28170-resistant promastigotes

Phytomonas serpens WT promastigotes were initially cultured in the presence of 5 μM MDL28170, a sublethal concentration of the drug corresponding to a sixth of the IC_{50} value (50% inhibitory concentration) to the WT cells (30·9 μM) (Oliveira *et al*. 2017). A stepwise increase in drug concentration was undertaken only when the drug-exposed promastigotes had a growth rate similar to those of the WT culture. This process was applied until the final concentration of 70 μM MDL28170 was reached. Resistant parasite cells (MDL^R) were maintained under constant drug pressure by cultivating in Warren medium plus 70 μM MDL28170 continuously. The IC_{50} of MDL^R population was determined by culturing parasites in the presence of the calpain inhibitor in the 70–140 μM range up to 96 h. The number of live promastigotes was evaluated under optical microscopy at 24-h intervals and the IC_{50} was determined after 48 h (mid-log growth phase). This value was assessed by linear regression analysis, by plotting the log number of viable promastigotes *vs* drug concentration by use of Origin Pro 7.5 computer software. The resistance index (the ratio of IC_{50} value for MDL^R and WT populations) was then calculated. In order to evaluate the persistence of the resistant phenotype, MDL^R population was cultured in a drug-free medium for a period of 6 months, after which the culture was again subjected to the presence of MDL28170 at final concentrations in the 10–70 μM range.

Cross-resistance to other calpain inhibitors

The determination of cross-resistance to calpain inhibitor V and PD150606 was carried out using the MDL^R population described above. Promastigote forms were washed in cold phosphate-buffered saline (PBS; 150 mM NaCl, 20 mM phosphate buffer, pH 7·2) prior to resuspension in the drug-free Warren medium to yield 10^6 cells mL^{-1}. Drug solutions of calpain inhibitor V and PD150606 were then added so as to obtain the 10–70 μM concentrations range. The number of live promastigotes was evaluated under optical microscopy

https://doi.org/10.1017/S0031182017001561 Published online by Cambridge University Press

at 24-h intervals and the IC_{50} values were determined after 48 h, as described above.

Parasite viability analysis

Resazurin dye/AlamarBlue® (7-hydroxy-3H-phenoxazin-3-one 10-oxide) and MTT [3-(4,5-dimethylthiazol-2-yl)-2,5-diphenyltetrazolium bromide] were employed for promastigote viability testing. Assays were performed in sterile 96-well plates using WT and MDL^R *P. serpens* promastigotes. For the resazurin assay, 20 μL of a solution containing 0·0125% resazurin (w/v) in PBS were added to each well (containing 5×10^6 cells each), and plates were incubated for 4 h at 28 °C. After incubation, cells were analysed at a microplate reader (SpectraMax spectrofluorometer, Molecular Devices) using a pair of 590 and 544 nm as emission and excitation wavelengths, respectively. For the MTT assay, both populations (10^7 cells $well^{-1}$) were resuspended in fresh medium (200 μL) and MTT solution (5 mg mL^{-1} in PBS, 50 μg $well^{-1}$) was added. Plates were then incubated for 3 h in the dark at 37 °C. After centrifugation at 672 ***g*** for 7 min, the supernatant was removed, the pellet was dissolved in 200 μL of DMSO and absorbance was measured in the same microplate reader at 490 nm. In both experiments, parasites were also treated with sodium azide (0·95 g L^{-1}) for 30 min in order to obtain non-viable cells to use as a positive control.

In order to confirm cell membrane integrity, WT and MDL^R *P. serpens* promastigotes (5×10^6 cells) were washed twice in PBS and incubated with 10 μM propidium iodide (PI), a DNA-binding vital dye, for 30 min at room temperature, protected from light. The parasites were washed in PBS and their fluorescence was quantified on a flow cytometer (FACSCalibur, BD Bioscience, USA) equipped with a 15 mW argon laser emitting at 535 nm. As a control of dead cells, promastigotes were boiled for 20 min and then processed for PI staining as described above.

Cell morphology and ultrastructural analysis

Light microscopy evaluation was performed in order to detect possible alterations on parasite morphology between WT and MDL^R parasites. Parasites were stained with Giemsa and then observed in a Zeiss microscope (Axioplan, Oberkochen, Germany). By flow cytometry (FACSCalibur, BD Bioscience, USA), each experimental population was mapped by using a two-parameter histogram of forward-angle light scatter (FSC) *vs* side scatter (SSC) to measure two morphological parameters: cell size and granularity, respectively.

Ultrastructural analysis was also performed in WT and MDL^R cultures. For scanning electron microscopy observation, promastigotes were fixed for 40 min at 25 °C with 2·5% glutaraldehyde in 0·1 M cacodylate buffer, pH 7·2. After fixation, cells were washed in cacodylate buffer and post-fixed with a solution of 1% OsO_4, 0·8% potassium ferrocyanide and 5 mM $CaCl_2$ in the same buffer for 20 min at 25 °C. Cells were dehydrated in graded series of acetone (30–100%) and then dried by the critical point method, mounted on stubs, coated with gold (20–30 nm) and observed in a Jeol JSM 6490LV scanning electron microscope (Massachusets, USA) (Oliveira *et al*. 2017). For transmission electron microscopy observation, cells over coverslips were fixed and post-fixed as described above, dehydrated in an ascending acetone series and embedded in PolyBed 812 resin. Ultrathin sections were stained with uranyl acetate and lead citrate and examined in Jeol JEM1011 transmission electron microscope (Tokyo, Japan) at Plataforma de Microscopia Eletrônica, IOC, FIOCRUZ (Oliveira *et al*. 2017).

Expression of calpain-like, gp63-like and cruzipain-like proteins

WT and MDL^R *P. serpens* promastigotes (10^6 cells mL^{-1}) were fixed for 15 min in 0·4% paraformaldehyde in PBS (pH 7·2) at room temperature, followed by extensive washing in the same buffer. Alternatively, fixed cells were permeabilized by 0·01% Triton X-100 in PBS for 15 min at room temperature and then washed twice in PBS. The fixed and permeabilized cells maintained their morphological integrity, as verified by optical microscopic observation. Cells were then incubated for 1 h at room temperature with a 1:250 dilution of the following rabbit antibodies: anti-Dm-calpain (polyclonal, raised against the 70-kDa C-terminal region of calpain from *Drosophila melanogaster* and kindly donated by Dr Yasufumi Emori – Department of Biophysics and Biochemistry, Faculty of Sciences, University of Tokyo, Japan) (Emori and Saigo, 1994); anti-CAP5·5 (monoclonal, raised against the cytoskeleton-associated protein from *Trypanosoma brucei* and kindly provided by Dr Keith Gull – Sir William Dunn School of Pathology, University of Oxford, England) (Hertz-Fowler *et al*. 2001); anti-CDPIIb (polyclonal, raised against *Homarus americanus* calpains and kindly donated by Dr Donald L. Mykles – Colorado State University, USA) (Beyette *et al*. 1997); anti-gp63 (raised against the recombinant gp63 molecule from *Leishmania mexicana* and kindly provided by Dr Peter Overath – Max-Planck-Institut für Biologie, Abteilung Membranbiochemie, Germany) and anti-cruzipain (raised against cruzipain from *T. cruzi* and kindly provided by Dr Ana Paula C. A. Lima – Instituto de Biofísica Carlos Chagas Filho, Universidade Federal do Rio de Janeiro, Brazil). Cells were then incubated for an additional hour with a 1:100

https://doi.org/10.1017/S0031182017001561 Published online by Cambridge University Press

dilution of fluorescein isothiocyanate (FITC)-labelled goat anti-rabbit IgG (Sigma-Aldrich). Finally, cells were washed three times in PBS and analysed in a flow cytometry (FACSCalibur) equipped with a 15 mW argon laser emitting at 488 nm. Non-treated cells and those treated with the secondary antibody alone were run in parallel as controls (Oliveira *et al*. 2017).

WT and MDL^R *P. serpens* promastigotes (10^6 cells) were also fixed in paraformaldehyde and then processed as described for the flow cytometry analysis using a 1:250 dilution of the anti-gp63 antibody for the localization of gp63-like proteins by confocal fluorescence microscopy. In this set of experiments, the fixed cells maintained their plasma membrane integrity, as verified by PI labelling (described previously). Subsequently, cells were incubated with the FITC-labelled anti-IgG secondary antibody as well as with 4′,6-diamidino-2-phenylindole (DAPI) at 10 $\mu g\ \mu L^{-1}$ for 15 min to stain nucleus and kinetoplast. Cells were then washed three times in PBS and observed in a Leica TCS SP5 confocal microscope.

Alternatively, cruzipain-like proteins were detected by Western blotting. WT and MDL^R *P. serpens* promastigotes (2×10^8 cells) were collected by centrifugation at 3000 ***g*** for 5 min at 4 °C, washed three times with cold PBS and lysed with 100 μL of a buffer containing 125 mM Tris, pH 6·8, 4% sodium dodecyl sulphate (SDS), 20% glycerol, 1 mM β-mercaptoethanol and 0·002% bromophenol blue. Immunoblot analysis was performed with total cellular extracts (equivalent to 5×10^6 cells) as previously described (Oliveira *et al*. 2017). The secondary antibody used was peroxidase-conjugated goat anti-rabbit IgG at 1:25 000 followed by chemiluminescence immunodetection after reaction with ECL reagents. An anti-α-tubulin monoclonal antibody (Sigma-Aldrich) at 1:1000 dilution was also used as a control for sample loading in the immunoblot. The relative molecular mass of the reactive polypeptides was calculated by comparison with the mobility of SDS–PAGE standards and the densitometric analysis was performed using the ImageJ program.

Detection and measurement of calcium-dependent and calcium-independent cysteine peptidase activity

Calcium-dependent and calcium-independent cysteine peptidase activity over two fluorogenic substrates was determined using both WT and MDL^R promastigotes. Whole parasite cellular extracts were obtained by repeated freeze-thawing cycles of 10^7 viable cells in a buffer containing 70 mM imidazole, 2 mM dithiotreitol (DTT), 1% CHAPS [3-((3-cholamidopropyl)dimethylammonio)-1-propanesulfonate], pH 7·0. Then, the cellular extract was centrifuged at 10 000 ***g*** for 30 min at 4 °C, and the supernatant immediately used to determine the protein content and the proteolytic activity. The protein concentration was determined by the method described by Lowry *et al*. (1951), using bovine serum albumin (BSA) as standard. The cleavage of the fluorogenic substrates Z–Leu–Tyr–AMC (AMC = amidomethylcoumarin) and Z–Leu–Leu–Val–Tyr–AMC (Sigma-Aldrich), commonly used to measure calpain activity (Atsma *et al*. 1995), was monitored continuously in a spectrofluorometer (SpectraMax Gemini XPS, Molecular Devices, CA, USA) using an excitation wavelength of 380 nm and an emission wavelength of 460 nm. A 5-mM stock solution of each fluorogenic substrate was prepared in DMSO. The reaction was started by the addition of each substrate (20 μM) to the parasite extract (10 μg protein) in a total volume of 60 μL of a buffer containing 70 mM imidazole, 2 mM DTT, 1% CHAPS, pH 7·0, in the presence or in the absence of 100 mM calcium chloride. In this set of experiments, MDL28170 at 10 μM, the cysteine peptidase inhibitor E-64 [*trans*-epoxysuccinyl L-leucylamido-(4-guanidino) butane] at 10 μM and the calcium chelator EGTA (ethylene glycol tetraacetic acid) at 1 mM were also used. The reaction mixture was incubated at 37 °C for 1 h. The assays were controlled for self-liberation of the fluorophore over the same time interval.

In parallel, the hydrolysis of the fluorogenic substrate Z–Phe–Arg–AMC (Sigma-Aldrich), commonly used to detect *T. cruzi* cruzipain activity (Cazzulo *et al*. 1990), was also measured using both populations. Whole parasite cellular extracts were obtained as described above. The reaction was started by the addition of the fluorogenic substrate (20 μM, starting from a 5-mM stock solution in DMSO) to the parasite extract (10 μg protein) in a total volume of 60 μL of 50 mM sodium phosphate buffer, pH 5·0, containing 2 mM DTT, in the absence or in the presence of 10 μM E-64. The reaction mixture was incubated at 37 °C for 1 h. The assays were also controlled for self-liberation of the fluorophore over the same time interval.

Cysteine peptidase activities were also assayed in gelatin-containing SDS-PAGE (Heussen and Dowdle, 1980). WT and MDL^R promastigotes were washed three times in PBS and then lysed by the addition of 0·1% SDS. Cells were broken in a vortex by alternating 1-min shaking and 2-min cooling intervals, followed by centrifugation at 10 000 ***g*** for 30 min at 4 °C, in order to obtain the whole-parasite cellular extracts. Samples containing 50 μg of protein of each system were resuspended in 125 mM Tris, pH 6·8, 4% SDS, 20% glycerol and 0·002% bromophenol blue. After electrophoresis at a constant voltage of 120 V at 4 °C, SDS was removed by incubation with 10 volumes of 2·5% Triton X-100 for 1 h at room temperature under constant agitation. Then, the gels were incubated at 37 °C in 50 mM sodium phosphate buffer supplemented with 2 mM DTT, pH 5·0, for 48 h, to

https://doi.org/10.1017/S0031182017001561 Published online by Cambridge University Press

promote the proteolysis. The molecular masses of the peptidases were estimated by comparison with the mobility of low molecular mass standards.

Phytomonas serpens – O. fasciatus salivary glands interaction

A milkweed bug (*O. fasciatus*) culture kit was purchased from Carolina Biological Supply Company, Burlington, North Carolina, USA. These insects originated the colony maintained at Laboratório de Bioquímica de Microrganismos (Instituto de Microbiologia Paulo de Góes, UFRJ, Brazil). Adult *O. fasciatus* insects (Hemiptera: Lygaeidae) were kept in plastic pitchers under a 12 h light/dark cycle at 28 °C with 70–80% relative humidity and fed with peeled and toasted sunflower seeds and distilled water (Romeiro *et al*. 2000). WT and MDL^R *P. serpens* promastigotes (10^7 cells) were cultured in Warren medium and then cells were washed three times in cold PBS, resuspended in PBS (5×10^6 cells in 100 μL) and added to dissected salivary glands (five per group). The parasites were allowed to bind for 1 h at room temperature in PBS. After the interaction period, the salivary glands were extensively washed with PBS, individually transferred to microcentrifuge tubes containing 50 μL of PBS and homogenized (Oliveira *et al*. 2017). The released trypanosomatids were counted in a Neubauer chamber. The results are shown as the mean ± standard error of the mean (S.E.M.) of three experiments.

Intracellular accumulation of Rhodamine 123

The accumulation of the fluorochrome dye Rhodamine 123 (R123) is inversely related to the amount of efflux pumps present on the surface of the parasite (Forster *et al*. 2012), and it was explored in the present paper in order to identify one of the possible mechanisms involved in the resistance of MDL^R cells to the calpain inhibitor MDL28170. In addition, the calcium channel blocker verapamil and the immunosuppressant cyclosporin A, known to reverse multidrug resistance (Xiong *et al*. 2015), were also used.

First, WT and MDL^R promastigotes of *P. serpens* (5×10^6 cells mL^{-1}) in the log-phase of growth were incubated at 28 °C in Warren medium in the presence and in the absence of cyclosporin A (50 μM) or verapamil (50 μM) for 2 h at 28 °C. R123 (5 μg mL^{-1}) was then added, and the cells were incubated for 30 min at 28 °C. Cells were then washed three times in PBS, resuspended with PBS and their fluorescence was quantified on a flow cytometer (FACSCalibur) equipped with a 15 mW argon laser emitting at 488 nm. In parallel, cells were mounted on 0·2 M *n*-propylgallate in glycerol:PBS (9:1) and the fluorescence images were acquired using appropriated filters in a Zeiss epifluorescence microscope (Axioplan 2).

Statistical analysis

All experiments were performed in triplicate, in three independent experimental sets. The data were analysed statistically by means of Student's *t* test using EPI-INFO 6.04 (Database and Statistics Program for Public Health) computer software. *P* values of 0·05 or less were considered statistically significant.

RESULTS

Selection of MDL28170-resistant promastigotes of P. serpens

In order to generate a population of *P. serpens* promastigotes displaying MDL28170 resistance, WT cells were initially cultured in the presence of sublethal concentrations of this calpain inhibitor and a stepwise increase in its concentration was performed. After approximately 6 months, the culture was resistant to the concentration of 70 μM MDL28170 (MDL^R population). The construction of a comparative growth curve between WT and MDL^R populations of *P. serpens* showed that MDL^R cells presented a proliferation rate in the presence of 70 μM MDL28170 comparable with the WT population (Fig. 1A). The doubling time of WT and MDL^R populations were 9 h 28 min and 9 h 45 min, respectively. This drug concentration inhibited WT parasite growth by approximately 85% after 48 h (Fig. 1A). The kinetics of growth pattern of MDL^R in the presence of higher concentrations of MDL28170 was then investigated, and a dose-dependent reduction in the proliferation rate was observed (Fig. 1B). The IC_{50} value for MDL^R culture was determined as 115·4 μM after 48 h of growth. For comparison, the IC_{50} value for the WT culture in the same time interval was determined as 30·9 μM (Oliveira *et al*. 2017), and as such the resistance index for MDL^R population was calculated as 3·7.

In order to test the *in vitro* stability of the resistance phenotype, MDL^R cells of *P. serpens* were subcultured in the drug-free Warren medium for 6 months (MDL^S population), and then subjected to susceptibility assays in the presence of MDL28170. The effect of the calpain inhibitor in MDL^S population was intermediary between WT and the original MDL^R population: the IC_{50} value of MDL28170 for MDL^S promastigotes was calculated as 66·7 μM after 48 h of growth, with a reduction in the resistance index to 2·2 (Fig. 1C).

Cross-resistance to other calpain inhibitors

The *in vitro* susceptibility of *P. serpens* WT population to the calpain inhibitors V and PD150606 was previously determined and the IC_{50} values calculated as 32·3 and 42·8 μM, respectively (Oliveira

https://doi.org/10.1017/S0031182017001561 Published online by Cambridge University Press

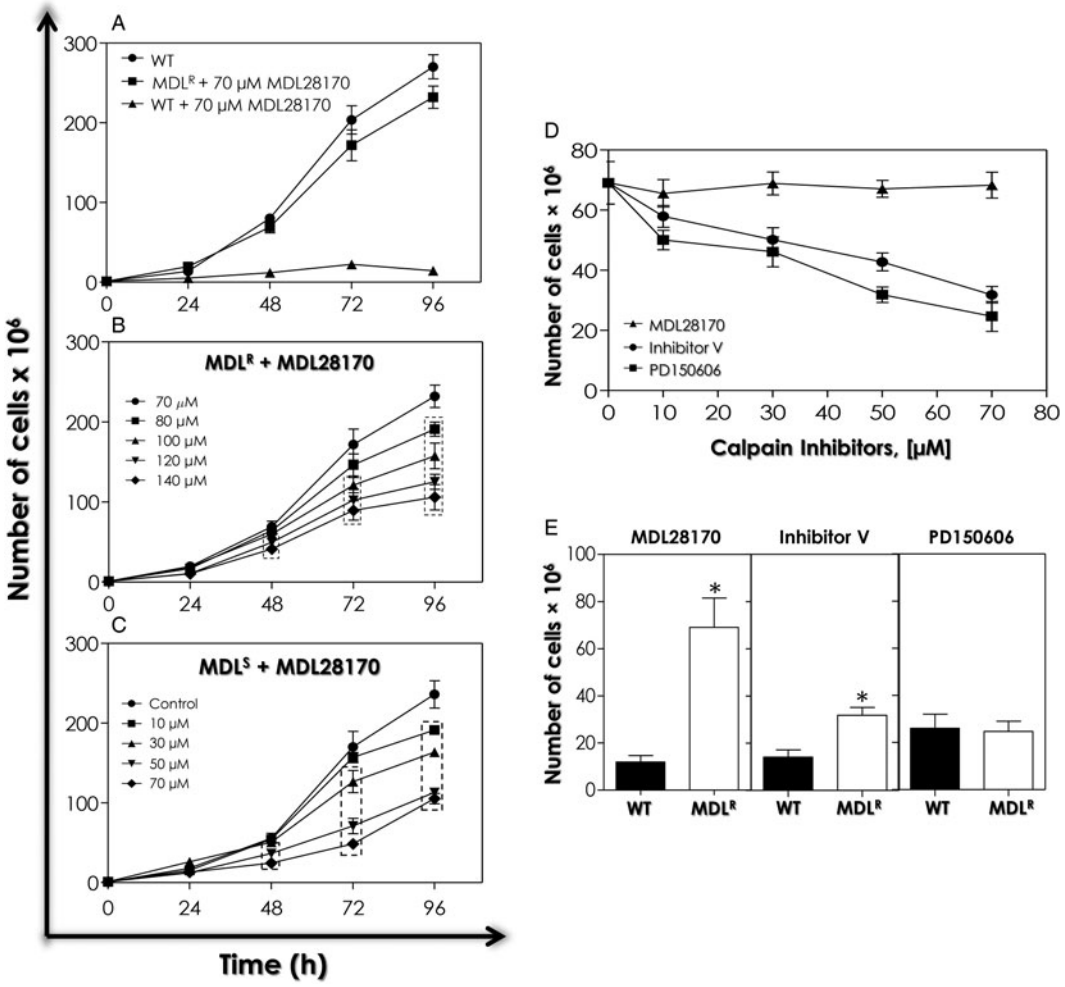

Fig. 1. Growth profile and effect of calpain inhibitors on the growth rate of MDL28170-resistant (MDL^R) promastigotes of *P. serpens*. (A) Comparative growth curve of the wild-type (WT) population, in the absence or in the presence of 70 μM MDL28170, and MDL^R cells plus 70 μM MDL28170. (B) Effect of MDL28170 on the proliferation rate of MDL^R promastigotes. (C) Evaluation of the stability of resistance of MDL^R population. Cells kept for six months in the absence of the calpain inhibitor (MDL^S cells) were cultured in the presence or absence (control) of MDL28170. (D) (MDL^R) promastigotes were cultured in the presence of the calpain inhibitors V and PD150606 for 48 h in concentrations ranging from 10 to 70 μM. (E) Comparison of the number of WT and MDL^R cells in the presence of each calpain inhibitor at 70 μM after 48 h of growth. Data shown represent the mean ± standard deviation of three independent experiments performed in triplicate. The dotted boxes in (B and C) highlight growth rates significantly different from control ($P < 0{\cdot}05$). The asterisks denote statistic difference to control ($P < 0{\cdot}05$).

et al. 2017). For MDL^R population, the IC_{50} values of the same calpain inhibitors were determined after 48 h (Fig. 1D). For calpain inhibitor V, the IC_{50} value was calculated as 65·9 μM, which is approximately twice as that determined for the WT population, being suggestive of cross-resistance of MDL^R population for this inhibitor. On the other hand, no cross-resistance was found to the calpain inhibitor PD150606, since the IC_{50} value for the MDL^R culture was 49·5 μM, which is very close to the one previously determined to the WT promastigotes. In order to further explore this result, a comparison of the proliferation rate of *P. serpens* WT and MDL^R populations was performed in cells pre-treated with either 70 μM MDL28170 or 70 μM calpain inhibitor V for 48 h (Fig. 1E). It was possible to observe that proliferation was 5·8- and 2·2-fold lower in WT cells, respectively, when compared with the proliferation rate of MDL^R cells cultured during the same time interval, which confirms the cross-resistance to both calpain inhibitors. In contrast, WT and MDL^R promastigotes pretreated with 70 μM PD1500606 presented a similar proliferation rate (Fig. 1E).

Cell viability

Parasite viability in MDL^R population was confirmed using the resazurin and MTT assays, which showed similar levels of fluorescence and absorbance signals, respectively, to WT cells (Fig. S1A and B). This result indicated that the

https://doi.org/10.1017/S0031182017001561 Published online by Cambridge University Press

selection of the resistant population did not induce loss of parasite viability. Incubation with azide showed a reduction in cell viability when compared with WT and MDL^R populations (Fig. S1A and B).

WT and MDL^R *P. serpens* cells were also incubated in the presence of PI in order to compare plasma membrane integrity. Analysis by flow cytometry indicated no change in plasma membrane permeability in MDL^R parasites when compared with WT promastigotes (Fig. S1C and D), in contrast to the positive control of cell death.

Morphological and ultrastructural analysis

Flow cytometry, light microscopy, scanning and transmission electron microscopy techniques were employed in order to evaluate the morphology and ultrastructure of *P. serpens* MDL^R population. Analysis by flow cytometry showed that WT and MDL^R cells presented similar cell size and granularity, as revealed by FSC and SSC parameters, respectively (Fig. S2A). Corroborating this result, both light microscopy (Fig. S2A, inset) and scanning electron microscopy (Fig. S2B) revealed no morphological differences between both populations, showing the typical *P. serpens* promastigote morphology, like an elongated cell body and a single, long flagellum (Fig. S2A inset and S2B), besides an anterior kinetoplast in relation to the nucleus (Fig. S2A, inset). These results are in accordance to the similar growth rate and viability of both populations (Fig. 1A, Fig. S1). MDL^R promastigotes apparently presented an increased amount of small vesicles in the parasite surface (Fig. S2B).

When the ultrastructure of these parasites was compared by transmission electron microscopy, no significant changes were found between WT (Fig. S2C-a and b) and MDL^R (Fig. S2C-c–e) populations: the typical morphology of nucleus, mitochondrion, kinetoplast and flagellar pocket of promastigotes was observed. However, the presence of microvesicles within the flagellar pocket of MDL^R promastigotes and in the culture supernatant was detected (Fig. S2C-e, inset).

Expression of cysteine peptidases

Our next goal was to evaluate the expression/activity of cysteine peptidases in both populations in order to compare the cruzipain-like proteolytic activity previously detected by our group in WT cells (Santos *et al*. 2007) and, simultaneously, to detect calpain-like proteins whose expression could be affected in MDL^R promastigotes. At first, the activity of calcium-dependent cysteine peptidases was compared using two substrates commonly used for detection of calpain activity: Z–Leu–Tyr–AMC and Z–Leu–Leu–Val–Tyr–AMC. Our data showed that the soluble extract of WT and MDL^R cultures of *P. serpens* was able to cleave both calpain substrates at similar rates in the absence of calcium (Fig. 2A).

When calcium was added to the reaction mixture, an increase of 158% was found for the hydrolysis of Z–Leu–Tyr–AMC in WT cells, while for MDL^R soluble extract the increase was by 75% (Fig. 2A). Under these conditions, the addition of the highly selective cysteine peptidase inhibitor E-64 or the calpain inhibitor MDL 28170 inhibited the hydrolytic activity at similar levels: by 88 and 91%, respectively, in the soluble extract of WT, and by 85 and 87%, respectively, in the soluble extract of MDL^R population (Fig. 2A). When the calcium chelator EGTA was included in the reaction mixture, the reduction of the substrate hydrolysis was by 74 and 78% in WT and MDL^R cells, respectively (Fig. 2A). These results suggest the predominance of hydrolysis of Z–Leu–Tyr–AMC by calcium-dependent cysteine peptidases.

The hydrolysis rate for Z–Leu–Leu–Val–Tyr–AMC was also raised for WT soluble cellular extract in the presence of calcium, although at minor levels (78%), while for MDL^R population no significant change in hydrolysis was detected (Fig. 2A). Similarly, E-64, EGTA and MDL28170 inhibited the hydrolytic activity on both cellular extracts in the presence of calcium: in WT population, the reduction in the hydrolysis of this substrate was 83, 64 and 88%, respectively; MDL^R soluble extract presented an inhibition of 71, 57 and 73%, respectively, in the hydrolytic ability of the substrate (Fig. 2A).

A more detailed kinetics analysis confirmed the results described above: the addition of calcium to the assay buffer reduced the K_m values for both substrates in the soluble extract of WT and MDL^R cultures of *P. serpens* (Table S1). In addition, K_m values were higher for Z–Leu–Tyr–AMC when compared with Z–Leu–Leu–Val–Tyr–AMC, and for MDL^R population in comparison with WT cells (Table S1). E-64 and MDL28170 were also evaluated as inhibitors of calcium-dependent cysteine peptidases activity against both substrates. In our assay, the calculated apparent inhibition constants (K_i values) for E-64 were found to be lower in both substrates when compared with MDL28170, which exhibited the highest K_i values. The values of K_i calculated for both inhibitors in the MDL^R population were at least two times higher than that of WT cells (Table S2).

Previously, our group found by Western blotting analysis in WT cells that anti-Dm-calpain antibody reacted with three polypeptide bands migrating at approximately 80, 70 and 50 kDa, while a single 50-kDa polypeptide was detected with anti-CAP5·5 and anti-CDPIIb antibodies. In that work, pre-treatment of *P. serpens* WT cells with

https://doi.org/10.1017/S0031182017001561 Published online by Cambridge University Press

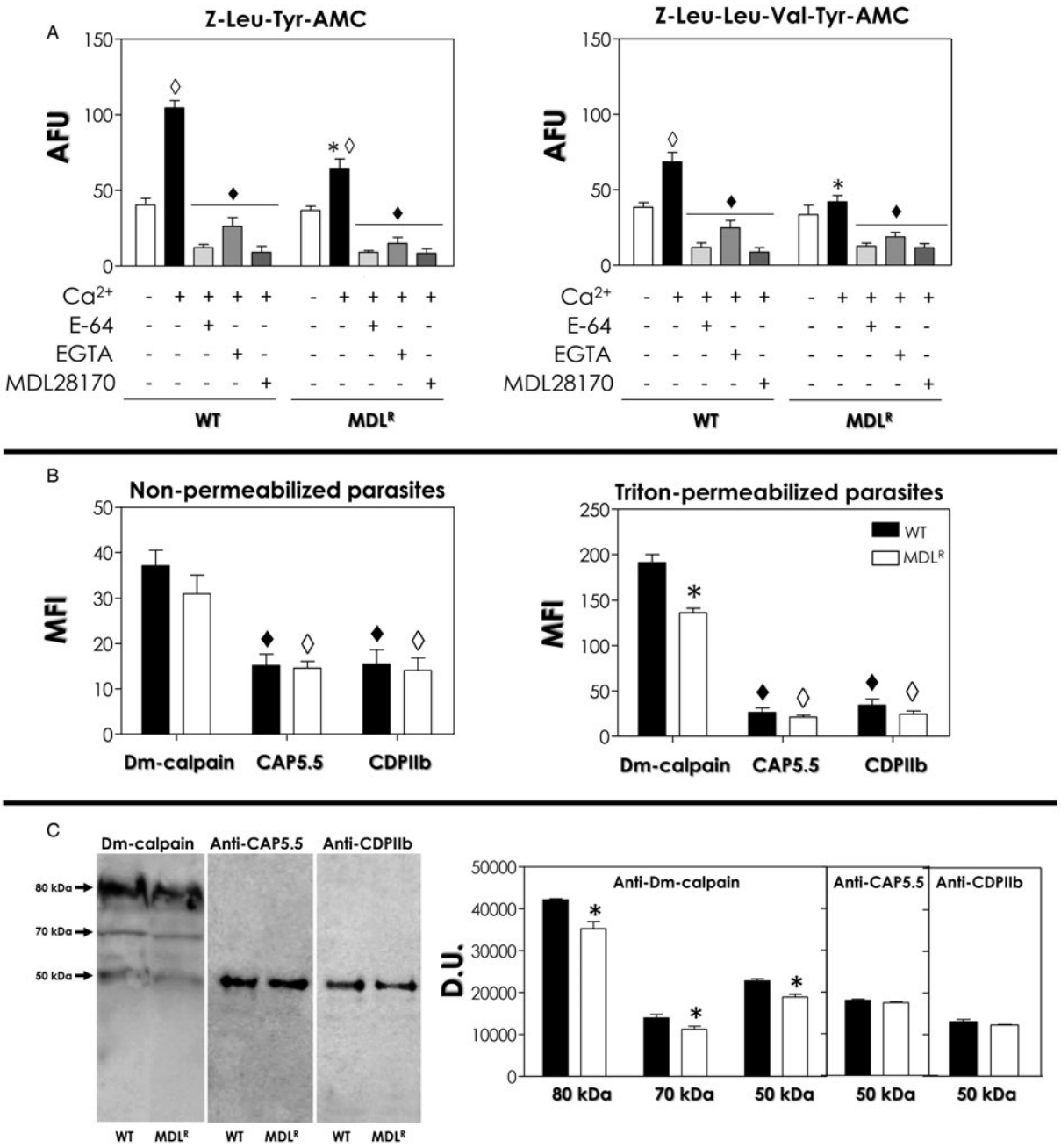

Fig. 2. Detection of calcium-dependent cysteine peptidase activities (A) and calpain-like proteins (B, C) in wild-type (WT) and MDL28170-resistant (MDL^R) promastigotes of *P. serpens*. (A) The whole cellular extract of each population was incubated with the fluorogenic substrates Z–Leu–Tyr–AMC and Z–Leu–Leu–Val–Tyr–AMC in the absence (– Ca^{2+}) or in the presence (+ Ca^{2+}) of calcium chloride, E-64, EGTA and MDL28170. The results were expressed as arbitrary fluorescence units (AFU). The values represent the mean ± standard deviation of three independent experiments performed in triplicate. The diamonds highlight the significant differences in each population in the presence or in the absence of calcium (*white*) or each modulator of calpain activity (*black*); the asterisks, between WT and MDL^R cells in the presence of calcium ($P < 0{\cdot}05$). (B) Fixed cells of each population, permeabilized or not, were incubated in the presence of anti-Dm-calpain, anti-CDPIIb and anti-CAP5·5 antibodies and then analysed by flow cytometry. Representative data of the analysis of 10 000 cells are shown and expressed as the mean fluorescence intensity (MFI). The asterisk highlights significantly different MFI levels between WT and MDL^R promastigotes after incubation with anti-Dm-calpain antibody, while diamonds denote significant differences in MFI values between labelling with anti-CAP5·5 and anti-CDPIIb antibodies in comparison with anti-Dm-calpain antibody in WT (black diamonds) and MDL^R cells (white diamonds). Labelling of permeabilized cells was significantly different from non-permeabilized cells for each of the three anti-calpain antibodies tested ($P < 0{\cdot}05$), and consequently the scale for MFI levels in each graph was different. (C) Western blotting showing the CALPs recognized in the whole cellular extract of each population by the anti-calpain antibodies. Anti-tubulin monoclonal antibody was used as a control for sample loading in the blots, revealing a protein band of 50 kDa in similar amount in both populations (not shown). The apparent molecular masses, expressed in kilodaltons, of each detected band are shown. Right panel, the densitometric analysis of the reactive bands detected in Western blotting is expressed as densitometric units (DU). The results represent means standard deviation of three independent experiments, and the asterisks denote statistic difference between WT cells and MDL^R promastigotes ($P < 0{\cdot}05$).

https://doi.org/10.1017/S0031182017001561 Published online by Cambridge University Press

the IC_{50} value of MDL28170 led to a reduction in the expression of epitopes reactive to anti-Dm-calpain, anti-CAP5·5 and anti-CDPIIb antibodies, indicating that calpain-like molecules are potential targets of the calpain inhibitor (Oliveira *et al*. 2017). A search for Dm-calpain, CAP5·5 and CDPIIb homologous proteins in the streamlined genome of *Phytomonas* sp. isolate EM1 (Porcel *et al*. 2014) was performed, and confirmed the presence of at least one calpain-conserved domain as well as the theoretical molecular mass consistent with the recognition by each antibody (Oliveira *et al*. 2017). Although the genome of *P. serpens* isolate 9T is available in Genbank, the genes have not been identified and no protein was predicted. Even so, in the present work a search for *P. serpens* sequences that could encode proteins homologous to the fragments employed to generate each antibody used in this work was performed on *t*Blastn. The *P. serpens* whole-genome shotgun sequence (WGS) AIHY01000314·1 encodes a calpain-like sequence of around 94 kDa capable of being recognized by anti-Dm-calpain and anti-CDPIIb antibodies (31 and 28% of amino acid identity, respectively). In addition, 17 homologues of the *T. brucei* CAP5·5 were found in *P. serpens* genome, eight of them with the conserved domain CysPc (pfam:Peptidase_C2) of the classical calpains. Moreover, two sequences (AIHY01001500·1 and AIHY01001547·1) presented a predicted molecular mass of 50 kDa, which supports the recognition of *P. serpens* 50-kDa CALP (31 and 26% identity, respectively). One of these sequences (AIHY01001500·1) is also homologous to the *H. americanus* CDPIIb and could be the same calpain-like molecule recognized by this antibody, displaying 31% identity. There also other ten homologous sequences in *P. serpens* genome that can be recognized by anti-CDPIIb antibody, although the predicted molecular mass do not support the experimental recognition by this antibody. These data encouraged us to evaluate the expression of CALPs in *P. serpens* MDL^R promastigotes.

Flow cytometry analysis of WT and MDL^R promastigotes of *P. serpens* was then performed using the three anti-calpain antibodies from distinct origins and different specificities in order to check for the differential expression of CALPs. In the present study, the highest MFI values were detected in the cross-reactivity with anti-Dm-calpain antibody, both at the cell surface as well as in the intracellular milieu, when compared with the binding of anti-CAP5·5 and anti-CDPIIb antibodies (Fig. 2B). The binding of the three anti-calpain antibodies was significantly enhanced when control, fixed cells were permeabilized, which indicates that CALPs cross-reactive to these antibodies are located mainly in intracellular compartments, especially for anti-Dm-calpain antibody, for which the increase was 416% for WT population and 338% for MDL^R population (Fig. 2B). Furthermore, the expression of intracellular molecules cross-reactive to anti-Dm-calpain antibody was significantly lower (approximately 30%) in MDL^R promastigotes when compared with WT cells, while the reactivity of the same antibody in the cell surface as well as anti-CAP5·5 and anti-CDPIIb antibodies was not altered (Fig. 2B). No significant difference in the percentage of fluorescent cells between WT and MDL^R promastigotes was observed in non-permeabilized and permeabilized cells (data not shown). Interestingly, the same polypeptide bands detected previously in WT population by Western blotting (Oliveira *et al*. 2017) were also detected In MDL^R population, but a significant reduction in the expression (in the 15–21% range) was observed only for the bands cross-reactive with anti-Dm calpain antibody, which confirmed the flow cytometry result (Fig. 2C).

The next step of the present study was to detect papain-like cysteine peptidase activity in *P. serpens* WT and MDL^R promastigote cells. Previous studies from our group have already identified and characterized the presence of two cell-associated cysteine peptidases at 38 and 40 kDa in *P. serpens* displaying cross-reactivity to the well-known cruzipain, the major cysteine peptidase from *T. cruzi* (Santos *et al*. 2007; d'Ávila-Levy *et al*. 2014). Our results from Western blotting analysis showed that MDL^R cells presented a significantly increased expression of the 38 and 40-kDa proteins that cross-reacted with anti-cruzipain antibody, in comparison with the expression in WT cells, by 32 and 58%, respectively (Fig. 3A and B). The cruzipain used to produce the anti-cruzipain antibody have 59% of amino acid identity with *P. serpens* isolate 9T WGS AIHY01001722·1, which could encode a 44-kDa protein and also have the cruzain domain. Concomitantly, the cell-associated proteolytic profile detected by gelatin–SDS–PAGE at pH 5·0 revealed the presence of two bands migrating at the same molecular masses in both populations, besides the detection of two proteolytic activities at 42 and 45 kDa (Fig. 3C). The latter bands had their expression increased in MDL^R cells (Fig. 3C). The quantification of the proteolytic activity against Z–Phe–Arg–AMC, a fluorogenic substrate commonly used to detect cysteine peptidase activity, including cruzipain (Cazzulo *et al*. 1990), was then tested. Confirming the results detected in gelatin–SDS–PAGE, MDL^R population presented a significant increase (27%) in the hydrolysis of the fluorogenic substrate when compared with WT cells (Fig. 3D). The addition of the cysteine peptidase inhibitor E-64 in the reaction mixture diminished significantly the hydrolytic activity in both systems by 80% (Fig. 3D).

https://doi.org/10.1017/S0031182017001561 Published online by Cambridge University Press

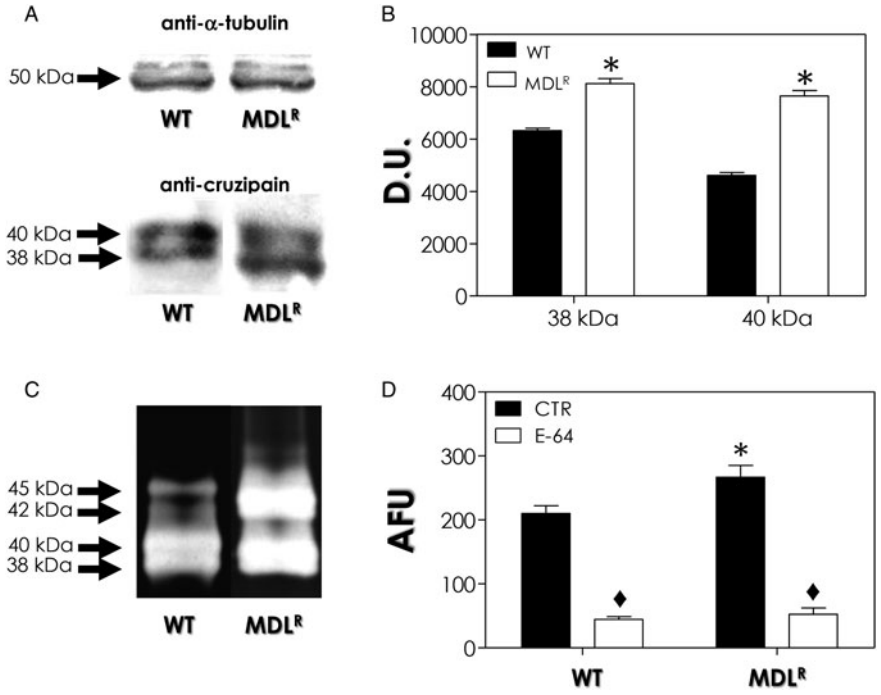

Fig. 3. Differential expression of intracellular cruzipain-like molecules and papain-like cysteine peptidase activity by wild-type (WT) and MDL28170-resistant (MDL^R) promastigotes of *P. serpens*. (A) Western blotting analysis showing the proteins recognized by the anti-cruzipain antibody. Anti-tubulin antibody was used as a control for sample loading. (B) The densitometric analysis of the reactive bands detected in Western blotting (A) is expressed as densitometric units (D.U.). (C) Peptidase profile analysis by gelatin–SDS–PAGE. The apparent molecular masses, expressed in kilodaltons, of each detected band in (A, C) are represented on the left. (D) The papain-like cysteine peptidase activity in parasites lysates was assessed by measuring the hydrolysis of Z–Phe–Arg–AMC in the absence (control, CTR) or the presence of E-64. Results are expressed as arbitrary fluorescence units (AFU). In (B, D), the values represent the mean ± standard deviation of three independent experiments performed in triplicate. The asterisks denote statistic difference between WT and MDL^R promastigotes, while diamonds highlight significant differences in the hydrolytic activity in the absence or the presence of E-64 ($P < 0{\cdot}05$).

Interaction with O. fasciatus salivary glands

Besides the evaluation of the expression of CALPs and cruzipain-like molecules in *P. serpens* WT and MDL^R cells, we also decided to study the expression of gp63-like molecules in these parasites. The rationale behind these experiments is the previous observation by our group that *P. serpens* expresses metallopeptidases that are related to *Leishmania* spp. gp63, which displays virulence-related functions in these pathogenic parasites (Santos *et al.* 2007). More importantly, *P. serpens* surface gp63-like proteins play an important role in the parasite adhesion to the salivary glands of the insect vector (Santos *et al.* 2007).

By flow cytometry, our results showed that the expression of molecules cross-reactive to anti-gp63 antibody in the surface of *P. serpens* MDL^R cells presented a reduction of 37% in the mean fluorescence intensity (MFI) value and of 46% in the percentage of fluorescent cells when compared with WT population (Fig. 4A). As previously described by our group (Santos *et al.* 2007), two polypeptides migrating in the 50–65 kDa range cross-react with anti-gp63 antibodies in *P. serpens* whole cellular extract. In the present work, Western blotting analysis showed the presence of both gp63-like protein bands; MDL^R cells presented a decreased expression of these proteins, in comparison with WT cells (Fig. 4A). The most expressed gp63 sequence of *L. mexicana* amastigotes (used to generate the anti-gp63 employed in the present work) have at least six homologues in *P. serpens* isolate 9T genome: AIHY01014097·1, AIHY01014205·1, AIHY01015147·1, AIHY01014315·1, AIHY01014400·1 and AIHY01014106·1, displaying 40–42% of amino acid identity. The predicted molecular mass of each one ranges from 44 to 59 kDa.

Our group has previously demonstrated the surface location of gp63-like molecules in *P. serpens* by agglutination assay, flow cytometry and immunofluorescence microscopy analyses (reviewed by Santos *et al.* 2007). In the present work, immunofluorescence microscopic images confirmed the surface location of gp63-like molecules in both populations and corroborated the reduction of expression in MDL^R parasites when compared with WT promastigotes (Fig. 4B). The next step was to verify whether MDL28170 resistance would influence the capacity of *P. serpens* to adhere to *O. fasciatus* explanted salivary glands: our results

https://doi.org/10.1017/S0031182017001561 Published online by Cambridge University Press

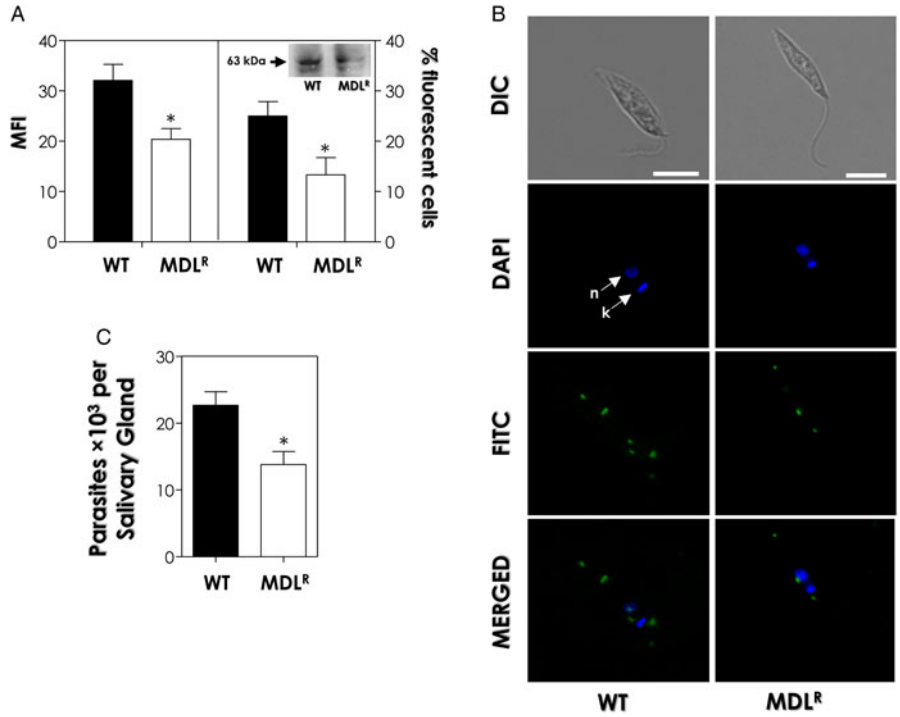

Fig. 4. Correlation between the expression of surface gp63-like molecules in wild-type (WT) and MDL28170-resistant (MDL^R) promastigotes of *P. serpens* and the interaction with the explanted salivary glands of *Oncopeltus fasciatus*. (A) Fixed promastigotes were incubated in the presence of anti-gp63 antibody and analysed by flow cytometry. The data are expressed as the mean of fluorescence intensity (MFI) levels and as the percentage of fluorescent cells (% FC). Representative data of the analysis of 10 000 cells in experiments performed in triplicate are shown and the results were considered significantly different when $P < 0{\cdot}05$ (*). In the inset, Western blotting showing the gp63-like proteins recognized in the whole cellular extract of each population by the anti-63 antibody. Anti-tubulin monoclonal antibody was used as a control for sample loading in the blots, revealing a protein band of 50 kDa in similar amount in both populations (not shown). The apparent molecular mass, expressed in kilodaltons, of the major band is shown. (B) Differential interference contrast microscopy (DIC) and immunofluorescence images showing the double labelling of *P. serpens* cells for gp63-like molecules cross-reactive to anti-gp63 antibody (FITC, green labelling) and DAPI (blue labelling). Below, the overlay of anti-gp63 and DAPI labelling. Bars: 5 μm. (C) Following interaction with each population, the salivary glands were washed and homogenized, and the released trypanosomatids were counted. The results are shown as the mean ± standard deviation of three independent experiments and the asterisk highlights significantly different values ($P < 0{\cdot}05$).

showed a significant reduction (38%) in the capacity of MDL^R cells to adhere to the salivary glands when compared with WT population (Fig. 4C).

Possible mechanism of resistance

By flow cytometry, our data showed that MDL^R cells presented a significant reduction (67%) in R123 accumulation in comparison with WT population (Fig. 5A). Since the efflux rate of R123 indicates the ability of the parasite to actively expel the drug from its body (Forster *et al*. 2012), it is possible to infer that efflux pumps may play a role MDL28170 resistance. In order to confirm this hypothesis, cells were pretreated with two inhibitors of ABC transporters, verapamil and cyclosporin A. First, the cytotoxicity of cyclosporin A and verapamil over the parasites was evaluated by colorimetric assay with resazurin, and the pretreatment of cells with both inhibitors up to the concentration of 50 μM was not capable of altering the viability of the parasites, when compared with untreated control cells (data not show). The pretreatment of WT and MDL^R cells with both inhibitors of efflux pumps led to a significant increase in the intracellular accumulation of R123, although with different intensities (Fig. 5A): the pretreatment of WT and MDL^R cells with verapamil led to an increase of 32·8 and 210·6%, respectively, whereas cyclosporin A increased by 37·5 and 225·7%, respectively, the intracellular accumulation of R123. For MDL^R cells, treatment with verapamil and cyclosporin A increased the MFI values to levels reaching the WT population (Fig. 5A).

In this same set of experiments, the capacity of *P. serpens* WT and MDL^R promastigotes to accumulate R123 was compared with MDL^R cells grown in the absence of the drug for 6 months (MDL^S population). By flow cytometry, our data showed that MDL^S population showed a 32% reduction in the MFI value when compared with WT promastigotes and an increase of 98·4% when compared with the

https://doi.org/10.1017/S0031182017001561 Published online by Cambridge University Press

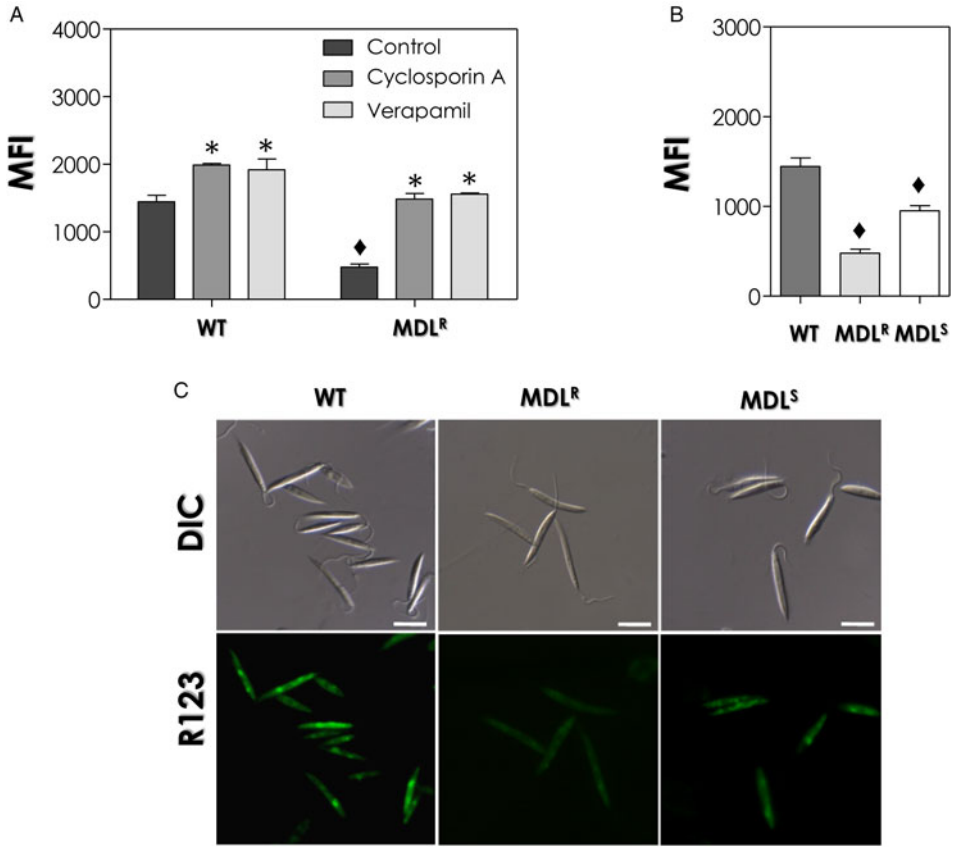

Fig. 5. Intracellular accumulation of rhodamine 123 (R123) in wild-type (WT) and MDL28170-resistant (MDL^R) promastigotes of *P. serpens*. The graphs in (A, B) represent the mean of fluorescence intensity (MFI) levels of intracellular accumulation of R123 analysed by flow cytometry. (A) WT and MDL^R cells were previously treated or not (control) with the ABC transporters inhibitors cyclosporin A and verapamil and subsequently incubated with R123. (B) WT and MDL^R cells accumulation of R123 was compared with the MDL28170-resistant population grown in the absence of MDL28170 for 6 months (MDL^S). The data presented in the graphs are representative of analysis of 10 000 cells in experiments performed in triplicate. The diamonds denote significant different values of accumulation of R123 between WT, MDL^R and MDL^S promastigotes, while the asterisks highlight significant different values in WT and MDL^R cells pretreated or not with ABC transporters inhibitors ($P < 0{\cdot}05$). (C) Differential interference contrast microscopy (DIC) and fluorescence microscopy of WT, MDL^R and MDL^S promastigotes showing the intracellular accumulation of R123. Bars: 5 μm.

resistant population (Fig. 5B), which indicates a partial reversion to the WT phenotype when compared with MDL^R promastigotes. In parallel to the flow cytometry analysis, cells were also observed under fluorescence microscopy, confirming the intermediary fluorescence of MDL^S cells between MDL^R and WT populations (Fig. 5C). Altogether, these data confirm the previous observation (Fig. 1C) that the effect of MDL28170 in the MDL^S population growth curve was intermediary between WT and the original MDL^R population.

DISCUSSION

There is not much information available about the roles of calpains and CALPs in trypanosomatids (Branquinha *et al*. 2013; Ennes-Vidal *et al*. 2017). It is worth mentioning that whole genome analysis characterized a large family of genes encoding CALPs in *T. brucei*, *T. cruzi* and *Leishmania major* (Ersfeld *et al*. 2005). Considering the high number of genes and sequence diversity of calpains in these parasites (Ersfeld *et al*. 2005), it is not an easy task to completely characterize this protein family and to assess its functions (Ennes-Vidal *et al*. 2017). Although there is no knockout available, the RNAi of three calpain genes in *T. brucei* revealed their roles in parasite growth, morphology and flagellum assembly (Olego-Fernandez *et al*. 2009; Hayes *et al*. 2014). Our group has been working with the feasible use of calpain inhibitors as leading compounds to search for new therapeutic options to treat trypanosomatid infections (Branquinha *et al*. 2013). Mechanisms of action of MDL28170 against *P. serpens* so far identified (Oliveira *et al*. 2017) include: effects on mitochondrion and *trans*-Golgi network; perturbation in processing of cruzipain-like molecules; repression of the activity of

https://doi.org/10.1017/S0031182017001561 Published online by Cambridge University Press

calcium-dependent cysteine-peptidases and expression of CALPs; and reduction in the interaction process with *O. fasciatus* salivary glands. Besides investigating the mechanism of action of MDL28170, it is fundamental to investigate the possibility of resistance to this calpain inhibitor in trypanosomatids, and that was the major goal of the present study. The biochemical analysis of the drug-resistant parasites was useful in trying to delineate the drug target(s) as well as the mechanisms developed by *P. serpens* promastigotes to reduce the lethal effect of MDL28170.

In this work, a viable population of *P. serpens* resistant to the calpain inhibitor MDL28170 at 70 μM (MDL^R population) was selected by culturing promastigotes in increasing concentrations of the drug. In trypanosomatids, the drug resistance phenotype is a complex physiological process, which is often polyclonal and involves several different co-existing genotypes in a given population. The heterogeneity in both genotype and phenotype in resistant populations may be either stable, being maintained in the absence of drug pressure, or unstable, and is therefore partially or totally lost when the parasite is kept in a drug-free medium (Vanaerschot *et al*. 2014). In the present work, the decrease in the resistance index in *P. serpens* MDL^S population (i.e., MDL^R cells subcultured in the drug-free Warren medium for 6 months) in comparison with MDL^R promastigotes indicates a partial reversion of MDL28170 susceptibility to the WT phenotype. However, it is important to note that the IC_{50} value of MDL^S promastigotes is still significantly higher than the IC_{50} of WT cells, which suggests that once any degree of resistance is achieved the culture does not revert back to the WT phenotype. Based on these data, the partial reversion in the resistance to MDL28170 in *P. serpens* MDL^S population observed in the present study may indicate the involvement of more than one molecular mechanism in the process of MDL28170 resistance, as will be discussed below. A more detailed genomic analysis may help to elucidate the possible pathways used by the parasite for protection against the effects of the drug.

Cross-resistance of *P. serpens* MDL^R population for calpain inhibitor V was also suggested by our results due to the increase in the IC_{50} value for the latter, although at lower levels. Differences in the degree of cross-resistance between MDL28170 and calpain inhibitor V might be explained by differences in the chemical structure, mechanism of action or specificity for a particular calpain structure (Donkor, 2015). Although MDL28170 and calpain inhibitor V are both active site-directed inhibitors, they have different chemical structures that have been developed for typical mammalian calpains. Consequently, we cannot exclude the possibility that these inhibitors act on similar targets in the trypanosomatid cell as well as on different targets. On the other hand, the calpain inhibitor PD150606 is specific for calcium-binding domains present in mammalian calpains that are essential for the enzymatic activity, which may explain the absence of cross-reactivity to MDL28170 (Wang *et al*. 1996). Although amino acid residues that are critical for calcium binding in mammalian calpains are partially conserved in some kinetoplastid sequences, these calcium-binding motifs are absent in trypanosomatid CALPs (Ersfeld *et al*. 2005). Analysis of these sequences revealed the presence of conserved domains, although residues critical for catalytic activity were frequently changed (Ersfeld *et al*. 2005).

MDL^R cells presented similar growth pattern and doubling time to WT promastigotes, and neither cell viability nor plasma membrane integrity were lost in the selection of the resistant population. Furthermore, no changes in the morphology and the typical ultrastructure of the parasites were visualized. These data provided supportive evidence that the experimental resistance selection was successful, adding the particular advantage that the parent WT cells and the derived MDL^R population could be directly compared for phenotypic analysis. The observation of microvesicles in the flagellar pocket of MDL^R promastigotes by transmission electron microscopy is suggestive of a possible drug sequestration for excretion, as observed in other drug-resistant trypanosomatids. For instance, when Engel *et al*. (2000) generated *T. cruzi* epimastigotes that were 20 times more resistant to a peptidomimetic cruzipain inhibitor than the WT, the secretory pathway was up-regulated in the resistant parasites due to the release of inactive cruzipain precursors complexed to the cysteine peptidase inhibitor. In a similar result to that observed in this study, transmission electron microscopy showed a multilamellar membrane-like material in the flagellar pockets of both amphothericin B-resistant *L. mexicana* amastigotes and promastigotes that was absent in WT cells (Al-Mohammed *et al*. 2005). These data are suggestive of similar responses of drug-resistant cells to the presence of drugs in the flagellar pocket, the site where endocytosis and exocytosis take place in trypanosomatids (Morgan *et al*. 2002).

In the present study, differences in CALPs expression and calcium-dependent cysteine peptidase activity between WT and MDL^R promastigotes were found. The reduced expression/activity of these molecules in MDL^R promastigotes may allow the parasite to survive in the presence of MDL28170. Indeed, the sub-expression of the target molecules of a drug has been reported in different trypanosomatids that have developed drug resistance. Yong *et al*. (2000) showed that *T. cruzi* epimastigotes (clone Dm28c) resistant to

https://doi.org/10.1017/S0031182017001561 Published online by Cambridge University Press

Z–(SBz)Cys–Phe–CHN_2, an irreversible cysteine peptidase inhibitor, presented significantly lower cysteine peptidase activity than that observed in parental cells, and this fact was accompanied by the reduced expression of cruzipain molecules, the major epimastigote cysteine peptidase, in the resistant parasites.

In contrast to the reduced calcium-dependent cysteine peptidase activity in *P. serpens* MDL^R promastigotes detected in this work, a higher expression of cruzipain-like molecules displaying papain-like cysteine peptidase activity was found in this population. A possible explanation to this difference may be found in *T. cruzi*. As previously mentioned, a *T. cruzi* population resistant to the cathepsin L-like cysteine peptidase inhibitor Z–(SBz)Cys–Phe–CHN_2 displayed a decreased cruzipain expression and a lower rate of cysteine peptidase fluorogenic substrate hydrolysis (Yong *et al*. 2000). Moreover, marked differences were seen in the protein profiles of *T. cruzi* resistant cells: the decreased expression of cruzipain was paralleled by the increased expression of a 30-kDa cysteine peptidase. This proteolytic activity was refractory to inhibition by Z–(SBz)Cys–Phe–CHN_2 and strongly recognized by anti-cathepsin B-like peptidase antibody, which indicated that the 30-kDa cysteine peptidase corresponds to a cathepsin B-like peptidase. This fact indicated that the deficit of metabolic functions promoted by inhibiting cruzipain was probably compensated by the increased expression of a cathepsin B-like target in *T. cruzi* (Yong *et al*. 2000). These results, besides the ones shown in the present work, may be correlated to the possible over-expression of distinct cysteine peptidase activities in order to compensate for the selection of cells resistant to cysteine peptidase inhibitors.

The induction of resistance may cause alterations in the expression of molecules involved in different cellular processes, as detected in this study for calpain-like and papain-like cysteine peptidases, and also virulence factors, which may affect the life cycle of the parasite. In addition, a reduced ability to replicate and/or cause disease is detected when a pathogen acquires drug resistance (Caljon *et al*. 2016). Several studies have shown that mutations that render pathogens resistant to drug treatment are likely to result in a loss of fitness, also defined as 'proficiency' (Caljon *et al*. 2016). In this sense, the lower levels of adhesion of MDL^R cells to *O. fasciatus* explanted salivary glands suggest that the fitness of the parasite might be affected in this population. The lower expression of gp63-like molecules in the cell surface of MDL^R promastigotes must be correlated to the reduced level of parasite adhesion to the invertebrate host, since these molecules were already described as potential adhesins expressed by the parasite to bind to salivary glands of phytophagous insects (d'Ávila-Levy *et al*. 2014).

Resistance to chemotherapy in trypanosomatids such as *Leishmania* spp. and *T. cruzi* is often caused by changes in the expression of membrane transport proteins (Campos *et al*. 2013; Yasinzai *et al*. 2013). Genome analysis of *Phytomonas* isolates EM1 and HART1 allowed the identification of 24 and 23 gene families, respectively, as belonging to the family of ABC transporters (Porcel *et al*. 2014). Although resistance to drugs is a complex phenomenon, the rate of efflux of the fluorescent dye R123 from the parasite cell, using flow cytometry, is an indication of the isolate's ability to efflux drugs, thus avoiding death, including trypanosomatids (Campos *et al*. 2013; Rai *et al*. 2013). In this sense, the lowest accumulation of the fluorochrome dye R123 detected in MDL^R promastigotes allowed us to assume that overexpression of efflux pumps is a possible mechanism of resistance developed by *P. serpens* MDL^R promastigotes. However, the R123 dye accumulation assay is considered less specific with respect to the transporter subtype activity, since dyes can be substrates of different ABC protein subtypes expressed in WT cells or native tissues (Cunha *et al*. 2017).

To investigate the phenomenon of multidrug resistance in *L. amazonensis*, it was demonstrated that the vinblastine-resistant phenotype was partially reverted by verapamil, which suggested that the cell line exhibited a multi-drug resistance phenotype. Confirming this assumption, R123 presented a lower intracellular accumulation in vinblastine-resistant cells due to an increased efflux (Gueiros-Filho *et al*. 1995). A similar profile was detected in *T. cruzi*: strains selected *in vitro* for the resistance to the compounds 4-N-(2-methoxy styryl)-thiosemicarbazone (2-Meotio) and benznidazole and then treated with R123 presented lower fluorescence than that exhibited by the parental line. Moreover, when the resistant lines were treated with cyclosporin A or verapamil, the fluorescence inside the resistant lines increased significantly, indicating the participation of efflux pumps in the process and, consequently, in the elimination of R123 by the resistant parasites (Campos *et al*. 2013). In the present work, the pretreatment of MDL^R cells with both inhibitors of efflux pumps, verapamil and cyclosporin A, led to a significant increase in the intracellular accumulation of R123 in comparison with WT cells, which confirmed the increase in the expression of ABC transporters in the resistant population.

Another aspect that deserves consideration is the increase in R123 accumulation in MDL^S cells when compared with MDL^R population and its reduction in comparison with WT cells. This may indicate that the partial reversion to the WT phenotype when MDL^R cells were cultured in a drug-free medium can be correlated to the reduced expression of membrane transporters. These data reinforce the

https://doi.org/10.1017/S0031182017001561 Published online by Cambridge University Press

previous observation that the partial reversion in the resistance to MDL28170 may indicate the involvement of more than one molecular mechanism in the process of MDL28170 resistance. Since no further decrease in resistance was observed in MDL^S cells and the resistance index in this population is still significantly higher than WT cells, the biochemical modifications described in the present paper in the resistant population may be stable, while others (such as the expression of ABC transporters) may be lost or reduced during the reversion process.

In conclusion, resistance to chemotherapy in a parasite reveals its gene plasticity and capability to adaptation to different environments. The stress caused by the presence of the drug probably leads to the selection of parasites with appropriate mechanisms to evade the lethal effects caused by antiparasitic compounds (Vanaerschot *et al*. 2014). In the present study, biochemical changes were observed that support the existence of more than one mechanism that act in concert to provide MDL28170 resistance in *P. serpens*. In this sense, the decreased expression of calpain-like molecules as well as calcium-dependent cysteine peptidase activity is, probably, a mechanism employed by *P. serpens* MDL^R cells to try to repeal the adverse effects of the continuous presence of the calpain inhibitor MDL28170. In contrast, the overexpression of cruzipain-like molecules, as well as the increase in its papain-like cysteine peptidase activity can be considered as a compensatory mechanism generated in MDL^R cells for the reduced presence of calcium-dependent cysteine peptidase activity. Induction of resistance to MDL28170 also significantly reduced the expression of gp63-like molecules, which is probably associated to the lowest ability of MDL^R promastigotes to interact with *O. fasciatus* salivary glands. This may indicate that the selection of the MDL28170-resistant population also affects the expression of molecules other than calpain-like or cysteine peptidases. However, we cannot affirm at the present moment that MDL28170 either has more than one target in trypanosomatids and may act in concert in the mechanisms cited above, or act sequentially in these processes. Additionally, the overexpression of efflux pumps in the cell surface of MDL^R promastigotes is suggestive of another possible mechanism of resistance developed by the parasite. Our study yielded notions about the multiplicity of mechanisms leading to MDL28170 resistance in *P. serpens* promastigotes.

SUPPLEMENTARY MATERIAL

The supplementary material for this article can be found at https://doi.org/10.1017/S0031182017001561.

ACKNOWLEDGEMENTS

The authors thank Denise da Rocha de Souza, who is supported by a FAPERJ fellowship, for technical assistance.

FINANCIAL SUPPORT

This work was supported by grants from the Brazilian Agencies: Conselho Nacional de Desenvolvimento Científico e Tecnológico (CNPq), Fundação de Amparo à Pesquisa no Estado do Rio de Janeiro (FAPERJ) and Fundação Coordenação de Aperfeiçoamento de Pessoal de Nível Superior (CAPES).

REFERENCES

Al-Mohammed, H. I., Chance, M. L. and Bates, P. A. (2005). Production and characterization of stable amphotericin-resistant amastigotes and promastigotes of *Leishmania mexicana*. *Antimicrobial Agents and Chemotherapy* **49**, 3274–3280.

Andrade, H. M., Murta, S. M., Chapeaurouge, A., Perales, J., Nirdé, P. and Romanha, A. J. (2008). Proteomic analysis of *Trypanosoma cruzi* resistance to benznidazole. *Journal of Proteome Research* **7**, 2357–2367.

Atsma, D. E., Bastiaanse, E. M., Jerzewski, A., Van der Valk, L. J. and Van der Laarse, A. (1995). Role of calcium-activated neutral protease (calpain) in cell death in cultured neonatal rat cardiomyocytes during metabolic inhibition. *Circulation Research* **76**, 1071–1078.

Beyette, J. R., Emori, Y. and Mykles, D. L. (1997). Immunological analysis of two calpain-like Ca^{2+}- dependent proteinases from lobster striated muscles: relationship to mammalian and *Drosophila* calpains. *Archives of Biochemistry and Biophysics* **15**, 337–341.

Branquinha, M. H., Marinho, F. A., Sangenito, L. S., Oliveira, S. S., Gonçalves, K. C., Ennes-Vidal, V., D'Avila-Levy, C. M. and Santos, A. L. (2013). Calpains: potential targets for alternative chemotherapeutic intervention against human pathogenic trypanosomatids. *Current Medicinal Chemistry* **20**, 3174–3185.

Brotherton, M. C., Bourassa, S., Leprohon, P., Légaré, D., Poirier, G. G., Droit, A. and Ouellette, M. (2013). Proteomic and genomic analyses of antimony-resistant *Leishmania infantum* mutant. *PLoS ONE* **8**, e81899.

Caljon, G., De Muylder, G., Durnez, L., Jennes, W., Vanaerschot, M. and Dujardin, J. C. (2016). Alice in microbe's land: adaptations and counter-adaptations of vector-borne parasitic protozoa and their hosts. *FEMS Microbiology Review* **40**, 664–685.

Campos, M. C., Castro-Pinto, D. B., Ribeiro, G. A., Berredo-Pinho, M. M., Gomes, L. H., da Silva Bellieny, M. S., Goulart, C. M., Echevarria, A. and Leon, L. L. (2013). P-glycoprotein efflux pump plays an important role in *Trypanosoma cruzi* drug resistance. *Parasitology Research* **112**, 2341–2351.

Cazzulo, J. J., Cazzulo Franke, M. C., Martínez, J. and Franke De Cazzulo, B. M. (1990). Some kinetic properties of a cysteine proteinase (cruzipain) from *Trypanosoma cruzi*. *Biochimica et Biophysica Acta* **1037**, 186–191.

Cunha, V., Burkhardt-Medicke, K., Wellner, P., Santos, M. M., Moradas-Ferreira, P., Luckenbach, T. and Ferreira, M. (2017). Effects of pharmaceuticals and personal care products (PPCPs) on multixenobiotic resistance (MXR) related efflux transporter activity in zebrafish (*Danio rerio*). *Ecotoxicology and Environmental Safety* **136**, 14–23.

d'Avila-Levy, C. M., Altoé, E. C., Uehara, L. A., Branquinha, M. H. and Santos, A. L. (2014). GP63 function in the interaction of trypanosomatids with the invertebrate host: facts and prospects. *Subcellular Biochemistry* **74**, 253–270.

Donkor, I. O. (2015). An updated patent review of calpain inhibitors (2012–2014). *Expert Opinion on Therapeutic Patents* **25**, 17–31.

Emori, Y. and Saigo, K. (1994). Calpain localization changes in coordination with actin-related cytoskeletal changes during early embryonic development of *Drosophila*. *Journal of Biological Chemistry* **269**, 25137–25142.

Engel, J. C., Torres, C., Hsieh, I., Doyle, P. S. and McKerrow, J. H. (2000). Upregulation of the secretory pathway in cysteine protease inhibitor-resistant *Trypanosoma cruzi*. *Journal of Cell Science* **113**, 1345–1354.

Ennes-Vidal, V., Menna-Barreto, R. F., Branquinha, M. H., Santos, A. L. S. and D'Avila-Levy, C. M. (2017). Why calpain inhibitors are interesting leading compounds to search for new therapeutic options to treat leishmaniasis? *Parasitology* **144**, 117–123.

Ersfeld, K., Barraclough, H. and Gull, K. (2005). Evolutionary relationships and protein domain architecture in an expanded calpain superfamily in kinetoplastid parasites. *Journal of Molecular Evolution* **61**, 742–757.

https://doi.org/10.1017/S0031182017001561 Published online by Cambridge University Press

Forster, S., Thumser, A. E., Hood, S. R. and Plant, N. (2012). Characterization of rhodamine-123 as a tracer dye for use in *in vitro* drug transport assays. *PLoS ONE* **7**, e33253.

Gueiros-Filho, F. J., Viola, J. P., Gomes, F. C., Farina, M., Lins, U., Bertho, A. L., Wirth, D. F. and Lopes, U. G. (1995). *Leishmania amazonensis*: multidrug resistance in vinblastine-resistant promastigotes is associated with rhodamine 123 efflux, DNA amplification, and RNA overexpression of a *Leishmania* mdr1 gene. *Experimental Parasitology* **81**, 480–490.

Hayes, P., Varga, V., Olego-Fernandez, S., Sunter, J., Ginger, M. L. and Gull, K. (2014). Modulation of a cytoskeletal calpain-like protein induces major transitions in trypanosome morphology. *Journal of Cellular Biology* **206**, 377–384.

Hertz-Fowler, C., Ersfeld, K. and Gull, K. (2001). CAP5·5, a life-cycle-regulated, cytoskeleton-associated protein is a member of a novel family of calpain-related proteins in *Trypanosoma brucei*. *Molecular and Biochemical Parasitology* **116**, 25–34.

Heussen, C. and Dowdle, E. B. (1980). Electrophoretic analysis of plasminogen activators in polyacrylamide gels containing sodium dodecyl sulphate and copolymerized substrates. *Analytical Biochemistry* **102**, 196–202.

Jaskowska, E., Butler, C., Preston, G. and Kelly, S. (2015). *Phytomonas*: trypanosomatids adapted to plant environments. *PLoS Pathogens* **11**, e1004484.

Lowry, O. H., Rosebrough, N. J., Farr, A. L. and Randall, R. J. (1951). Protein measurement with the Folin phenol reagent. *Journal of Biological Chemistry* **193**, 265–275.

Marinho, F. A., Gonçalves, K. C., Oliveira, S. S., Gonçalves, D. S., Matteoli, F. P., Seabra, S. H., Oliveira, A. C., Bellio, M., Oliveira, S. S., Souto-Padrón, T., d'Avila-Levy, C. M., Santos, A. L. and Branquinha, M. H. (2014). The calpain inhibitor MDL28170 induces the expression of apoptotic markers in *Leishmania amazonensis* promastigotes. *PLoS ONE* **9**, e87659.

Morgan, G. W., Hall, B. S., Denny, P. W., Carrington, M. and Field, M. C. (2002). The kinetoplastida endocytic apparatus. Part I: a dynamic system for nutrition and evasion of host defences. *Trends in Parasitology* **18**, 491–496.

Olego-Fernandez, S., Vaughan, S., Shaw, M. K., Gull, K. and Ginger, M. L. (2009). Cell morphogenesis of *Trypanosoma brucei* requires the paralogous, differentially expressed calpain-related proteins CAP5·5 and CAP5·5*V*. *Protist* **60**, 576–590.

Oliveira, S. S. C., Goncalves, D. S., Garcia-Gomes, A. S., Goncalves, I. C., Seabra, S. H., Menna-Barreto, R. F. S., Lopes, A. H. C. S., d'Avila-Levy, C. M., Santos, A. L. S. and Branquinha, M. H. (2017). Susceptibility of *Phytomonas serpens* to calpain inhibitors *in vitro*: interference on the proliferation, ultrastructure, cysteine peptidase expression and interaction with the invertebrate host. *Memórias do Instituto Oswaldo Cruz* **112**, 31–43.

Ono, Y. and Sorimachi, H. (2012). Calpains: an elaborate proteolytic system. *Biochimica et Biophysica Acta* **1824**, 224–236.

Porcel, B. M., Denoeud, F., Opperdoes, F., Noel, B., Madoui, M. A., Hammarton, T. C., Field, M. C., da Silva, C., Couloux, A., Poulain, J., Katinka, M., Jabbari, K., Aury, J. M., Campbell, D. A., Cintron, R., Dickens, N. J., Docampo, R., Sturm, N. R., Koumandou, V. L., Fabre, S., Flegontov, P., Lukeš, J., Michaeli, S., Mottram, J. C., Szöőr, B., Zilberstein, D., Bringaud, F., Wincker, P. and Dollet, M. (2014). The streamlined genome of Phytomonas spp. relative to human pathogenic kinetoplastids reveals a parasite tailored for plants. *PLoS Genetics* **10**, e1004007.

Rai, S., Bhaskar, E., Goel, S. K., Nath Dwivedi, U., Sundar, S. and Goyal, N. (2013). Role of efflux pumps and intracellular thiols in natural antimony resistant isolates of *Leishmania donovani*. *PloS ONE* **8**, e74862.

Rami, A., Ferger, D. and Krieglstein, J. (1997). Blockade of calpain proteolytic activity rescues neurons from glutamate excitotoxicity. *Neuroscience Research* **27**, 93–97.

Romeiro, A., Solé-Cava, A., Sousa, M. A., De Souza, W. and Attias, M. (2000). Ultrastructural and biochemical characterization of promastigote and cystic forms of *Leptomonas wallacei* n. sp. isolated from the intestine of its natural host *Oncopeltus fasciatus* (Hemiptera: Lygaeidae). *Journal of Eukaryotic Microbiology* **47**, 208–220.

Santos, A. L. S., D´Avila-Levy, C. M., Elias, C. G. R., Vermelho, A. B. and Branquinha, M. H. (2007). *Phytomonas serpens*: immunological similarities with the human trypanosomatid pathogens. *Microbes and Infection* **9**, 915–921.

Vanaerschot, M., Huijben, S., Van den Broeck, F. and Dujardin, J. C. (2014). Drug resistance in vectorborne parasites: multiple actors and scenarios for an evolutionary arms race. *FEMS Microbiology Review* **38**, 41–55.

Vergnes, B., Gourbal, B., Girard, I., Sundar, S., Drummelsmith, J. and Ouellette, M. (2007). A proteomics screen implicates HSP83 and a small kinetoplastid calpain-related protein in drug resistance in *Leishmania donovani* clinical field isolates by modulating drug-induced programmed cell death. *Molecular and Cellular Proteomics* **6**, 88–101.

Wang, K. K., Nath, R., Posner, A., Raser, K. J., Buroker-Kilgore, M., Hajimohammadreza, I., Probert, A. W., Marcoux, F. W., Ye, Q., Takano, E., Hatanaka, M., Maki, M., Caner, H., Collins, J. L., Fergus, A., Lee, K. S., Lunney, E. A., Hays, S. J. and Yuen, P. (1996). An alpha-mercaptoacrylic acid derivative is a selective nonpeptide cel-permeable calpain inhibitor and is neuroprotective. *Proceedings of the National Academy of Sciences USA* **93**, 6687–6692.

Xiong, J., Mao, D. A. and Liu, L. Q. (2015). Research progress on the role of ABC transporters in the drug resistance mechanism of intractable epilepsy. *BioMed Research International* **2015**, 194541.

Yasinzai, M., Khan, M., Nadhman, A. and Shahnaz, G. (2013). Drug resistance in leishmaniasis: current drug-delivery systems and future perspectives. *Future Medicinal Chemistry* **5**, 1877–1888.

Yong, V., Schmitz, V., Vannier-Santos, M. A., De Lima, A. P., Lalmanach, G., Juliano, L., Gauthier, F. and Scharfstein, J. (2000). Altered expression of cruzipain and a cathepsin B-like target in a *Trypanosoma cruzi* cell line displaying resistance to synthetic inhibitors of cysteine-proteinases. *Molecular and Biochemical Parasitology* **109**, 47–59.

https://doi.org/10.1017/S0031182017001561 Published online by Cambridge University Press